UC Berkeley
UC Berkeley Previously Published Works

Title

Discovery of sustainable drugs for Alzheimers disease: cardanol-derived cholinesterase inhibitors with antioxidant and anti-amyloid properties.

Permalink

Journal

Authors

de Andrade Ramos, Giselle
Souza de Oliveira, Andressa
Bartolini, Manuela
et al.

Publication Date

DOI

Peer reviewed

RSC
Medicinal Chemistry

rsc.li/medchem
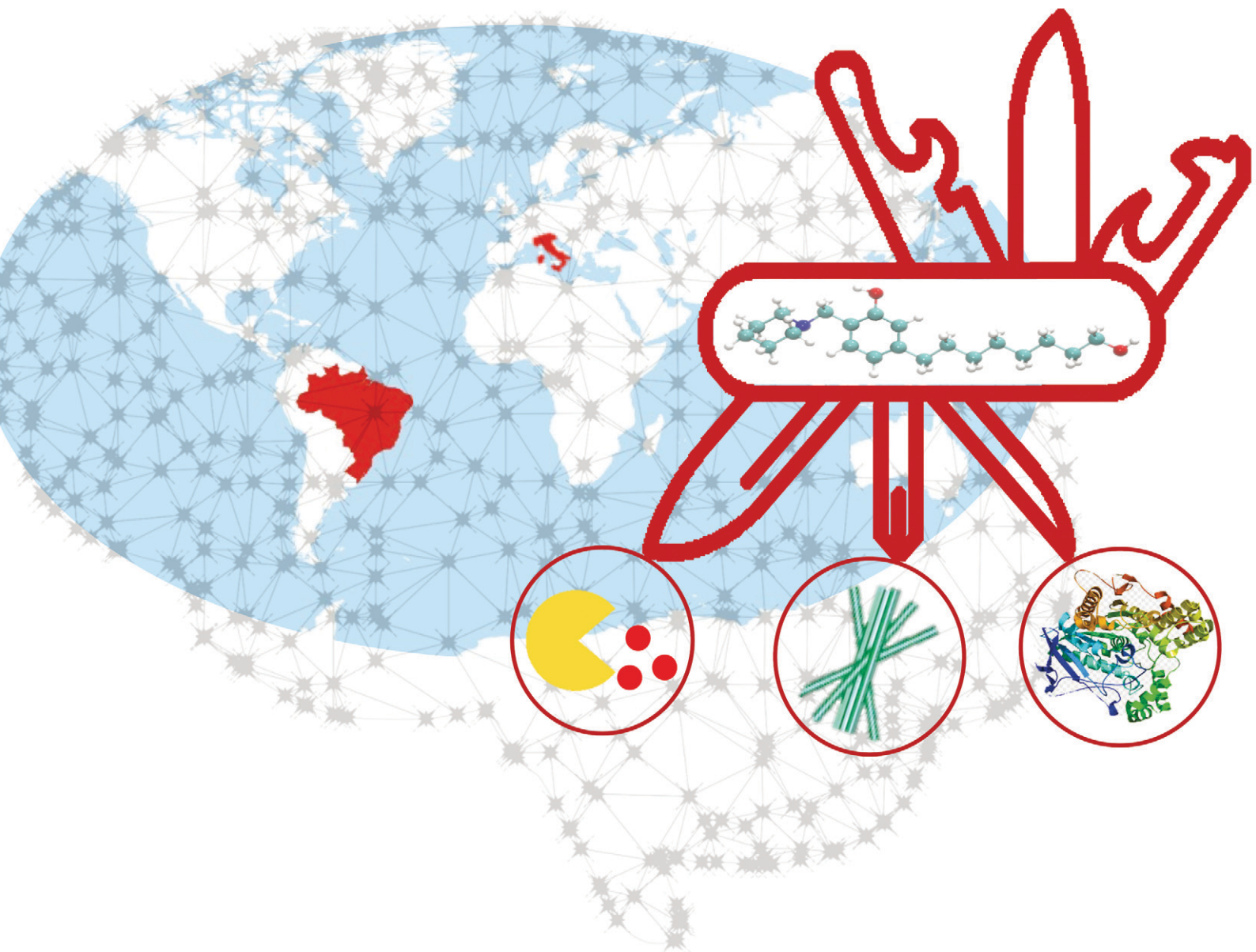
RESEARCH ARTICLE
Maria Laura Bolognesi, Luiz Antonio Soares Romeiro *et al.*
Discovery of sustainable drugs for Alzheimer's disease:
cardanol-derived cholinesterase inhibitors with antioxidant
and anti-amyloid properties

ROYAL SOCIETY
OF **CHEMISTRY**

Check for updates

Discovery of sustainable drugs for Alzheimer's disease: cardanol-derived cholinesterase inhibitors with antioxidant and anti-amyloid properties†

Giselle de Andrade Ramos,[a] Andressa Souza de Oliveira,[a] Manuela Bartolini,[b] Marina Naldi,[b] Irene Liparulo,[b] Christian Bergamini,[b] Elisa Uliassi, [b] Ling Wu,[c] Paul E. Fraser,[c] Monica Abreu,[d] Alessandra Sofia Kiametis,[d] Ricardo Gargano, [d] Edilberto Rocha Silveira,[e] Guilherme D. Brand,[f] Lukas Prchal,[g] Ondřej Soukup,[gh] Jan Korábečný,[gh] Maria Laura Bolognesi*[b] and Luiz Antonio Soares Romeiro [*a]

As part of our efforts to develop sustainable drugs for Alzheimer's disease (AD), we have been focusing on the inexpensive and largely available cashew nut shell liquid (CNSL) as a starting material for the identification of new acetylcholinesterase (AChE) inhibitors. Herein, we decided to investigate whether cardanol, a phenolic CNSL component, could serve as a scaffold for improved compounds with concomitant anti-amyloid and antioxidant activities. Ten new derivatives, carrying the intact phenolic function and an aminomethyl functionality, were synthesized and first tested for their inhibitory potencies towards AChE and butyrylcholinesterase (BChE). **5** and **11** were found to inhibit human BChE at a single-digit micromolar concentration. Transmission electron microscopy revealed the potential of five derivatives to modulate Aβ aggregation, including **5** and **11**. In HORAC assays, **5** and **11** performed similarly to standard antioxidant ferulic acid as hydroxyl scavenging agents. Furthermore, in *in vitro* studies in neuronal cell cultures, **5** and **11** were found to effectively inhibit reactive oxygen species production at a 10 μM concentration. They also showed a favorable initial ADME/Tox profile. Overall, these results suggest that CNSL is a promising raw material for the development of potential disease-modifying treatments for AD.

[a] *Department of Pharmacy, Health Sciences Faculty, University of Brasília, Campus Universitário Darcy Ribeiro, 70910-900, Brasília, DF, Brazil.*
E-mail: luizromeiro@unb.br

[b] *Department of Pharmacy and Biotechnology, University of Bologna, Via Belmeloro 6, 40126 Bologna, Italy. E-mail: marialaura.bolognesi@unibo.it*

[c] *Tanz Centre for Research in Neurodegenerative Diseases and Dept. of Medical Biophysics, University of Toronto, Krembil Discovery Tower, 60 Leonard Avenue, 6KD-402, M5T 2S8 Toronto, ON, Canada*

[d] *Physics Institute, University of Brasília, Campus Universitário Darcy Ribeiro, 70910-900, Brasília, DF, Brazil*

[e] *CENAUREMN, Department of Organic and Inorganic Chemistry, Federal University of Ceará, 60021-970, Fortaleza, CE, Brazil*

[f] *Chemistry Institute, University of Brasília, Campus Universitário Darcy Ribeiro, 70910-900, Brasília, DF, Brazil*

[g] *Biomedical Research Centre, University Hospital Hradec Kralove, Sokolska 581, 500 05 Hradec Kralove, Czech Republic*

[h] *Department of Toxicology and Military Pharmacy, Faculty of Military Health Sciences, University of Defence, Trebesska 1575, 500 01 Hradec Kralove, Czech Republic*

† Electronic supplementary information (ESI) available: Experimental procedures and characterisation for all compounds. Experimental details for biological assays and molecular modelling studies. See DOI: 10.1039/d1md00046b

Introduction

Alzheimer's disease (AD) has become a major global public health concern as the world population ages.[1] If increasing life expectancy is a triumph of the current society, it is sadly associated with a parallel increase in morbidity and disability due to age-related dementia. It is expected that by 2050, people aged >60 will account for 22% of the world's population, 80% of whom will be living in low- and middle-income countries.[2] Clearly, the growing population of older people at high risk in populous countries like Brazil and India makes AD and related dementia an even more complex problem than has been thought. This is particularly true in terms of access to therapies.

There is, therefore, an imperative need for low-cost drugs for use also in low- and middle-income countries.

Nowadays, cholinesterase inhibitors (ChEIs) remain the mainstay of AD therapy, with three currently available drugs approved by the U.S. Food and Drug Administration (FDA) (donepezil, galantamine, and rivastigmine) and one by the Chinese State Food and Drug Administration (SFDA) (huperzine A).[3] Although these drugs show limited clinical efficacy, with relatively short-lasting positive effects and no

Fig. 1 Methoxy–cardanol derivative LDT161 (**1**) obtained from a mixture of unsaturated cardanols (**12**).

disease-modifying activity, it is widely accepted that targeting central cholinesterases (ChEs) can temporarily mitigate cognitive decline in AD patients. In addition, recent evidence from neuroscientists, structural biochemists, clinicians, and neuropharmacologists makes ChEIs a class of drugs that still deserves attention for other potential positive effects against AD.[4]

As part of our efforts to develop sustainable AD drugs starting from the inexpensive and largely available cashew nut shell liquid (CNSL),[5,6] we recently reported on a methoxy–cardanol derivative (LTD161, **1**; Fig. 1) that exhibited a promising profile.[7]

In fact, thanks to the ability of interacting with both the catalytic active site (CAS) and the peripheral anionic site (PAS) of acetylcholinesterase (AChE) – thus acting as a dual binding inhibitor[8] – **1** showed a micromolar AChE activity.[7] In addition, **1** demonstrated positive features, such as a low toxicity and a favorable blood brain barrier (BBB) permeation prediction.

More importantly, it was obtained through simple synthetic steps from a bio-based, cheap, and inedible waste material. However, **1** was not able to prevent Aβ42 self-aggregation when tested at a 1/1 ratio. We speculated that this could be due to the methylation of the phenolic group of cardanol fragments (Fig. 1).[7]

To overcome the limitations of **1** and based on the knowledge of our and other's previous studies (see below), we designed and synthesized ten new derivatives (**2–11**; Fig. 2) that carry the intact phenolic structure of cardanol (**12**), together with additional functional moieties.

Our final aim was to develop new sustainable-by-design multifunctional derivatives that could combine the AChE inhibitory activity of **1** with other beneficial activities against AD, *i.e.*, anti-amyloid and antioxidant ones. The amyloid-cascade and the oxidative-stress hypotheses of AD have actually been united to one concept by many groups.[9–12] As such, combination makes sense from the AD pathogenesis point of view.[13] Accordingly, a plethora of ChEIs able to simultaneously target both cascades have been developed (see ref. 14 for a recent review and ref. 15 for a recent example). However, to best of our knowledge, there is no report dealing with this type of anticholinesterase/anti-amyloid/antioxidant molecule obtained from a waste material.

Along these lines, we aimed to transform **1** from a dual-binding AChE inhibitor into a sustainable and multifunctional cholinesterase inhibitor, with disease-modifying potential.[16]

Results and discussion

Design of target compounds 2–11

1 has been characterized as a dual-binding site inhibitor interacting with PAS through its aromatic end and fishing
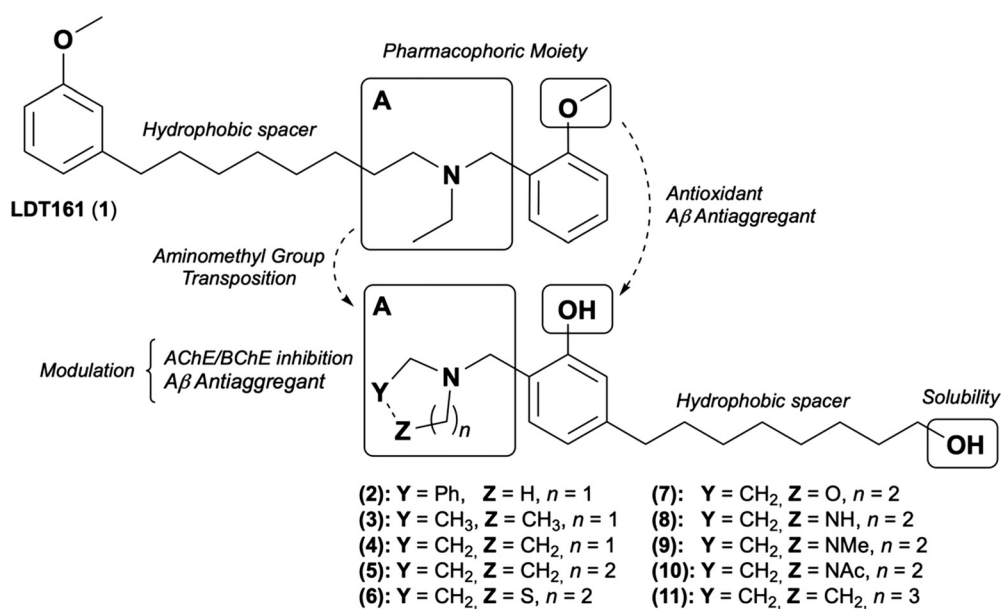
Fig. 2 Design rationale for cardanol derivatives **2–11**.

the CAS *via* the protonable amine function.[7] Towards the goal of expanding the anti-AD profile of **1** by including anti-amyloid/antioxidant activities, we properly manipulated the structure of **1** (Fig. 2).

First, we kept the free phenolic group of cardanol constant in all the target compounds. This was based on two reasons: (i) phenolic compounds, such as the red-wine polyphenol myricetin, the turmeric component curcumin, and its analogs rosmarinic acid and ferulic acid, inhibit the formation of Aβ aggregates, as well as dissociate preformed fibrils.[17,18] (ii) Phenol is the chemical moiety responsible of the radical scavenging activity of many phytochemicals that have been shown to be more effective antioxidants than vitamins E and C.[19] Furthermore, phenolic lipids, such as cardanol, have an even higher anti-oxidant potential due to the presence of a long side chain attached to the phenol ring.[20] The alkyl chain can stabilize oxidized molecules, thus hampering further radical formation. In addition, due to their lipophilicity, phenolic lipids can overcome limitations encountered with most small-molecule antioxidants: they can permeate the BBB and exert their central anti-oxidant effect.[20]

In parallel, we were inspired by the anti-amyloid activity of some recently reported Mannich bases.[21,22]

Furthermore, with respect to the C_{15} aliphatic chain of **12**, we used a shorter (C_8) homologue terminating with a primary alcoholic function (see general structure in Fig. 2). We have already reported that this modification positively modulates the excessive lipophilicity of our molecules and might reduce the potential surfactant properties.[23] In addition, the introduction of a terminal H-donor/acceptor (–OH) substituent might both improve the membrane permeability and allow establishing further H-bond interaction which might favor target(s) recognition.[23]

Collectively, we designed the set of cardanol derivatives **2–11** (Fig. 2), with the aim of obtaining sustainable ChEIs, with concomitant antioxidant and anti-amyloid properties.

Synthesis of target compounds 2–11

The designed series of derivatives (**2–11**) was prepared by Mannich aminomethylation of phenol **14** and benzyl, alkyl or heterocyclic amines as starting reagents (Scheme 1).

In detail, phenol **14** was synthesized using a three-step protocol. First, acetylation of a mixture of unsaturated cardanols (**12**), isolated from CNSL by following a procedure described by Paramashivappa *et al.*,[24,25] gave the corresponding acetylcardanol mixture **13** in 92% yield. Next, oxidative cleavage of **13** by ozonolysis, followed by the reduction of the resulting secondary ozonide to the corresponding primary alcohol with sodium borohydride furnished **14** in 60% yield. Subsequently, treatment of **14** with the respective iminium ions, previously formed from the reaction of paraformaldehyde with the suitable secondary amines, provided the target derivatives **2–11** with yields ranging from 32% to 81% (Scheme 1).

All compounds described herein possessed analytical and spectral data in agreement with the proposed structures.
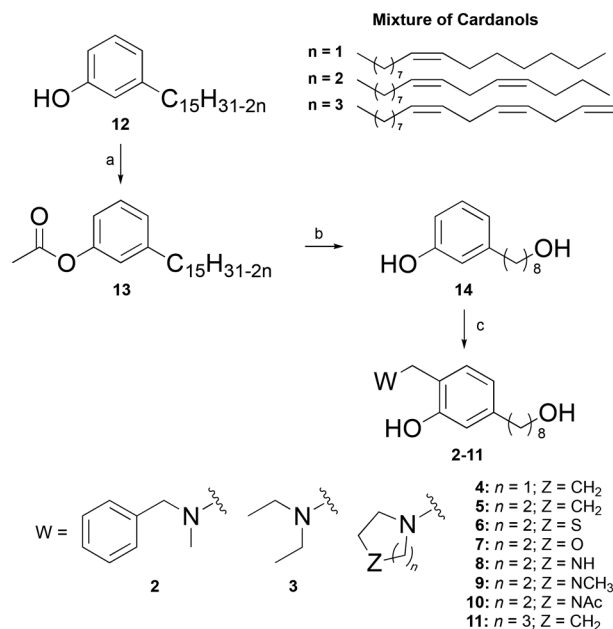
Scheme 1 Synthetic procedure for the synthesis of **2–11**. Reagents and conditions: (a) Ac_2O, H_3PO_4, MW irradiation 2.45 GHz, 270 W, 3 minutes, 92% (**13**); (b) i. O_3/O_2, dichloromethane/methanol 1:1, –70 °C, 1 h; ii. $NaBH_4$, 60% (**14**); (c) i. $(CH_2O)_n$, secondary amines, ethanol, reflux, 1.5 h; ii. **14**, reflux, 40 h, 32–81% (**2–11**).

Biological profile of the target compounds

AChE and BChE inhibitory activity. As the first step, the synthesized compounds **2–11** were tested for their ability to inhibit human AChE (hAChE) and BChE from human serum (hBChE) using the Ellman assay (Table 1).[26]

Essentially, most cardanol derivatives were devoid of AChE inhibitory activity when tested at 20 μM (% inhibition <20). In contrast, for pyrrolidine and piperidine derivatives **4** and **5**, the inhibition at 20 μM was 31.1% and 40.5%, respectively. The IC_{50} values for the inhibition of AChE by **4** and **5**, the most effective inhibitors of the current series, were 47.6 and 30 μM, respectively. Thus, the structural modification performed led to modest inhibitors, which were less active than **1** (IC_{50} = 5.65 μM), towards AChE inhibition.

More encouragingly, **2–11** were found to be fairly potent (and selective) regarding the inhibition of BChE. The presence of a benzyl amine (**1**), an open-chain diethylamine (**2**) or cyclic pyrrolidine (**4**), piperidine (**5**) or azepane (**11**) was associated with the best enzymatic profiles. The inhibition at 20 μM ranged from 50.5% for **3** to 77.1% for **11**. Conversely, the presence of thiomorpholine (**6**), morpholine (**7**), or piperazine (**8–10**) nuclei seems detrimental for BChE (% inhibition <20). The most potent and selective inhibitor was **11** (LDT692) (IC_{50} = 4.62 μM), which exhibits a similar inhibitory potency to reference drug donepezil against BChE (7.42 ± 0.39 μM).[27]

On the other hand, **4** and **5** emerged as dual AChE/BuChE moderate inhibitors: their activities against the two enzymes differ by 3.6 and 4.9 fold, respectively.

Table 1 Inhibitory activity against human AChE and BChE[a] and antioxidant activity toward hydroxyl radicals[b] of cardanol derivatives **2–11**

#	Code	W	% inhibition hAChE [I] = 20 μM	IC$_{50}$ hAChE (μM) ± SEM	% inhibition hBChE [I] = 20 μM	IC$_{50}$ hBChE (μM) ± SEM	HORAC Gallic acid equivalents
2	LDT544	benzyl-N-methylamino	19.4 ± 7.1	N.D.[d]	68.3 ± 1.3	6.74 ± 0.7	3.70 ± 0.05
3	LDT636	diethylamino	12.4 ± 1.2	N.D.[d]	50.5 ± 0.7	17.5 ± 3.5	5.49 ± 0.58
4	LDT637	pyrrolidin-1-yl	31.1 ± 2.8	47.6 ± 4.1	59.0 ± 0.8	13.3 ± 0.5	4.88 ± 0.05
5	LDT638	piperidin-1-yl	40.5 ± 1.8	30.0 ± 2.6	73.5 ± 0.4	6.12 ± 0.8	4.37 ± 0.54
6	LDT639	thiomorpholin-4-yl	12.1 ± 0.8	N.D.[d]	16.6 ± 2.4	N.D.[d]	4.38 ± 0.23
7	LDT640	morpholin-4-yl	<5	N.D.[d]	<10	N.D.[d]	9.73 ± 0.86
8	LDT641	piperazin-1-yl	<10	N.D.[d]	17.7 ± 3.1	N.D.[d]	1.49 ± 0.20
9	LDT642	4-methylpiperazin-1-yl	<5	N.D.[d]	10.6 ± 2.1	N.D.[d]	4.80 ± 0.49
10	LDT643	4-acetylpiperazin-1-yl	<10	N.D.[d]	<5	N.D.[d]	4.52 ± 0.64
11	LDT692	azepan-1-yl	<10	785 ± 42	77.1 ± 0.2	4.62 ± 0.14	3.50 ± 0.23
1	LDT161	n.a.[c]		5.65 ± 0.48			n.a.[c]
	Ferulic acid	n.a.[c]					4.04 ± 0.51
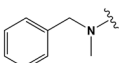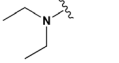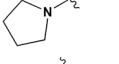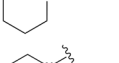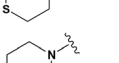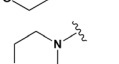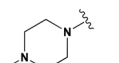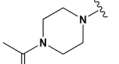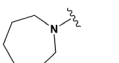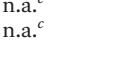
[a] IC$_{50}$ inhibitory concentration (μM) or % inhibition at 20 μM of human recombinant AChE and human serum BChE. IC$_{50}$ values are expressed as mean ± standard error of the mean (SEM) of at least two experiments each performed in triplicate. [b] Antioxidant activity is expressed as gallic acid equivalents (GAEs). GAE values are expressed as mean ± standard deviation (SD) of three experiments ($n = 3$). [c] n.a. = not applicable [d] N.D. = not determined.

The collected data can be interpreted positively in light of recent observations pointing to BChE as a more effective target than AChE for the treatment of dementia.[28] Several studies show a progressive reduction of AChE activity in AD patients, while BChE activity rises in response to the loss in hydrolysis capacity.[29] Furthermore, BChE inhibitors have been reported to improve animal cognition in scopolamine-treated and AD mouse models, indicating their value for the treatment of dementia from both Alzheimer's and other types.[30,31]

In summary, the structural manipulation of **1** proved successful only in terms of activity towards hBChE and only for selected compounds. Compounds carrying only one nitrogen atom in the cycle exhibit increasing selectivity toward BChE with increasing size of the cycle, reaching a value of approximately 170 for the seven-membered-ring **11**.

This is in agreement with the notion of the larger gorge of hBChE compared to that of hAChE,[32] which allows BChE to accommodate larger rings easier.

AChE and BChE docking studies. Aiming at investigating the binding modes of **2–11** and at an improved understanding of the experimental data, molecular docking simulations were performed using the crystal structures of hAChE[33] and hBChE[34] (PDB IDs: 4EY7 and 6EQP, respectively). To validate our protocol, we first carried out a redocking of donepezil to the hAChE binding site. In this procedure, the ligand superimposed the crystal within a RMSD <2 Å. Fig. 3 depicts the top scoring pose of each molecule in both cavities. Overall, **2–11** showed suitable conformational flexibility and length, spanning the PAS and the acyl-binding pocket (A-site) of the gorges. In particular, the molecules reached deeper into the hBChE gorge, also
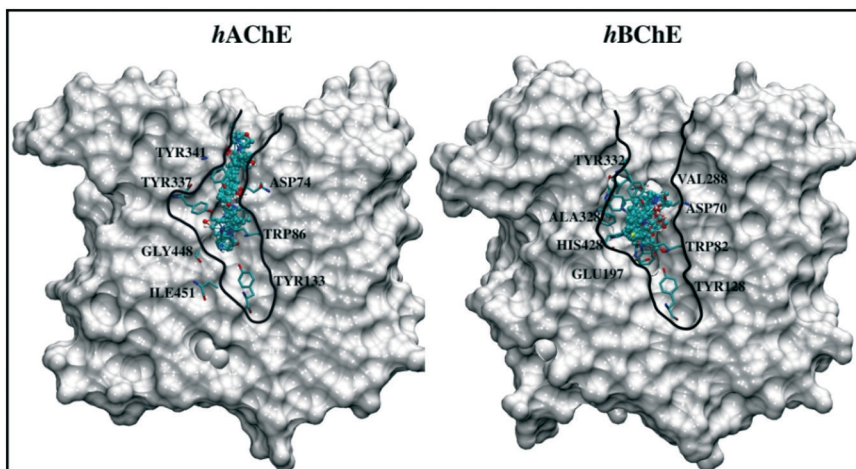
Fig. 3 Putative binding sites of **2**–**11** at human ChEs. In the case of *h*AChE, the molecules spanned the PAS (Tyr341, Asp74) and the A-site (Tyr337, Trp86) of the gorge. As they have no contact with the CAS, the molecules are not dual binding inhibitors. In the case of *h*BChE, the molecules spanned the PAS (Tyr332, Asp70) and the A-site (Trp82), and also spanned the CAS (His428) as they are quite flexible.

spanning the CAS. *h*BChE has a larger active site gorge than *h*AChE, due to the presence of a valine and a leucine instead of the bulkier phenylalanines of *h*AChE. As **2**–**11** are quite flexible, there was a trend of finding solutions mostly buried in the CAS. On the other hand, in the case of *h*AChE, molecules were confined at the PAS and A-site not in contact with the CAS. This finding suggests that the molecules are not dual binding, accounting for their low inhibitory percentages against *h*AChE.

Fig. 4 and 5 depict the putative binding modes of the most active cholinesterase inhibitors, *i.e.*, **5** (LDT638) and **11** (LDT692) at both enzymes. Inside the *h*AChE gorge, **5** can form π-stacking interactions with residues Tyr341 (PAS) and Trp86 (A-site) *via* its phenol and piperidine groups, respectively. Hydrogen bonds can be formed with residues Tyr124 and Asp74 (PAS) *via* its protonated nitrogen. Also, **5** makes additional favorable contacts with Trp286 (PAS) and Phe338 (A-site) *via* aromatic hydrophobic interactions. In the
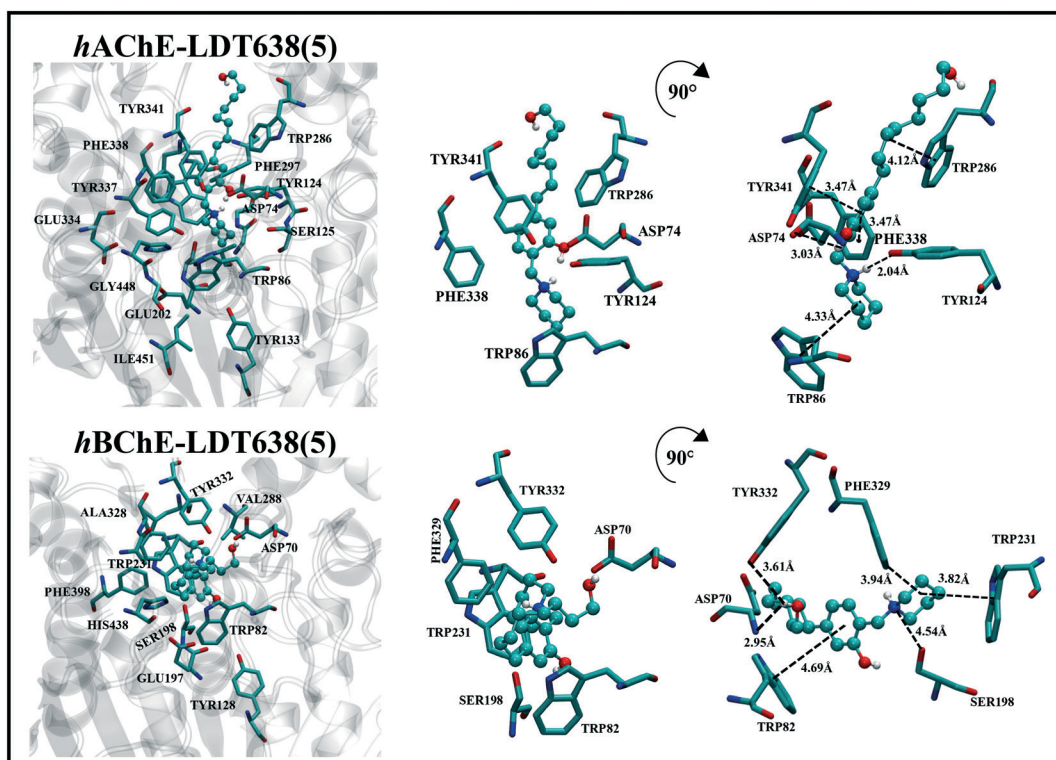
Fig. 4 Putative binding modes of LDT638 (**5**) with *h*AChE and *h*BChE.
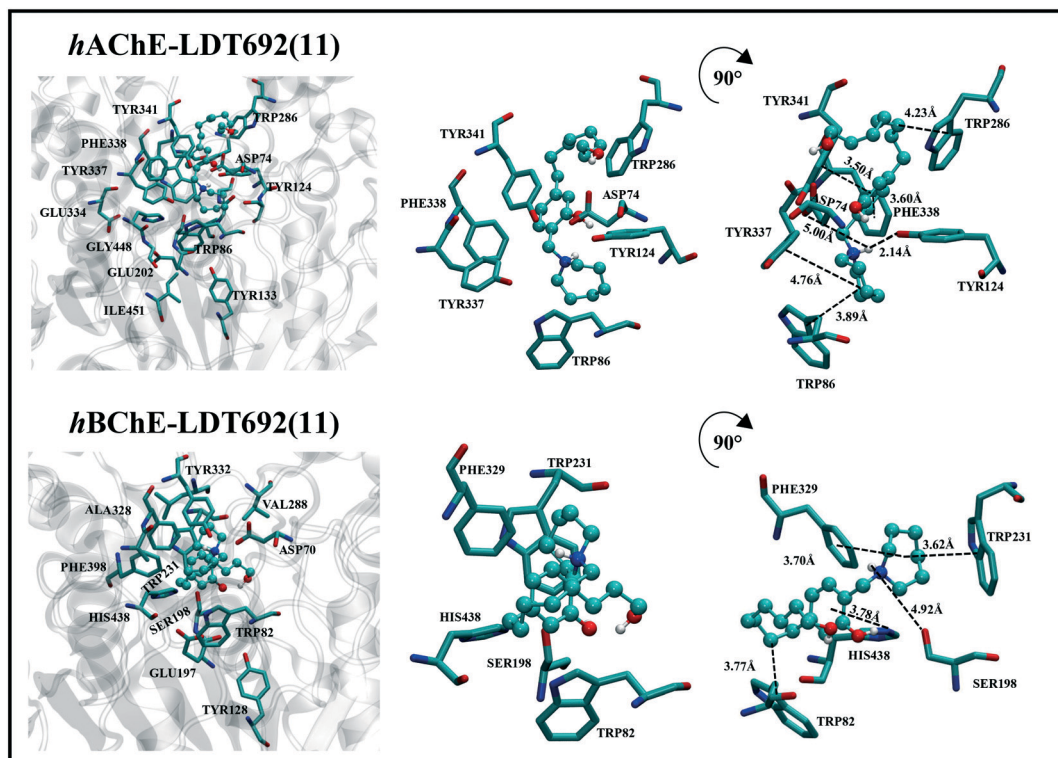
Fig. 5 Putative binding modes of LDT692 (11) with hAChE and hBChE.

complex with hBChE, 5 can form hydrogen bonds with Ser198 (CAS) and Asp70 (PAS), via its protonated nitrogen and hydroxyl groups, respectively. Furthermore, 5 can form a π-stacking interaction with Trp82 (A-site) via its phenol group and a t-stacking interaction between residue Trp231 (A-site) and the piperidine group. Finally, 5 makes close contacts with residues Tyr332 (PAS) and Phe329 (A-site).

As for the putative binding mode of 11 at the hAChE gorge (Fig. 4), the molecule can form multiple π-stacking interactions: in the A-site (Phe338, Tyr337, Trp86) via its azepine group, or in the PAS (Tyr341), via its phenol group. Hydrogen bonds can be formed with residues Tyr124 and Asp74 (PAS) via its protonated nitrogen, similar to 5. 11 makes additional favorable contacts with Trp286 (PAS) via aromatic hydrophobic interaction. When complexed with hBChE, it can establish π-stacking and t-stacking interactions with residues Phe329 (A-site) and Trp231 (PAS), respectively, via its azepane group. In addition, 11 makes close contacts with Trp82 (A-site) via aromatic hydrophobic interaction. The possibility of hydrogen bonds with residues Ser198 and His438 of CAS may support its higher inhibitory potency against hBChE.

In vitro anti-amyloid profile

To explore the anti-amyloid profile of 2–11, peptide Aβ42 was used. Specifically, fibril formation in the absence and in the presence of cardanol derivatives was examined by transmission electron microscopy (TEM). Since TEM can probe amyloid fibrils at the molecular level, it is widely used to qualitatively assess the impact of tested compounds on the Aβ fibril overall abundance and morphology.[35]

To this end, samples of Aβ42 at 65 μM were stained and visualized at t = 0 and after 48 h incubation with and without 2–11. The occurrence and morphology of Aβ aggregates were inspected.

Fig. 6 shows that after 48 h incubation at 37 °C, large fibrillar assemblies could be observed only in control samples containing Aβ42 alone, whereas in the presence of the selected inhibitors (2, 3, 5, 7 and 11), small and rather amorphous aggregates are evident. Thus, we could infer that 2, 3, 5, 7 and 11 interfere with the formation of organized Aβ42 fibrils, promoting amorphous, non-toxic aggregates.

In the past, most of Aβ-targeting strategies focused on the disassembly of Aβ fibrils or inhibition of Aβ fibril formation. However, these strategies have been questioned as a decrease in fibrillar content would lead to an increased concentration of the more toxic soluble species of Aβ.[36] Alternatively, phenolic derivative (−)-epigallocatechin-3-gallate (EGCG) seems to modulate Aβ activity by forcing the peptide to deviate from the conventional fibrillar architecture in favor of off-pathway amorphous globular aggregate states that have been found to be benign in toxicity.[37] It has been further suggested that the formation of these non-toxic amorphous aggregates could be additionally beneficial as they would function as potential sinks for soluble Aβ oligomers.[38]

Likely, phenols 2–11 could similarly stimulate the formation of globular aggregates over fibrillar structures.
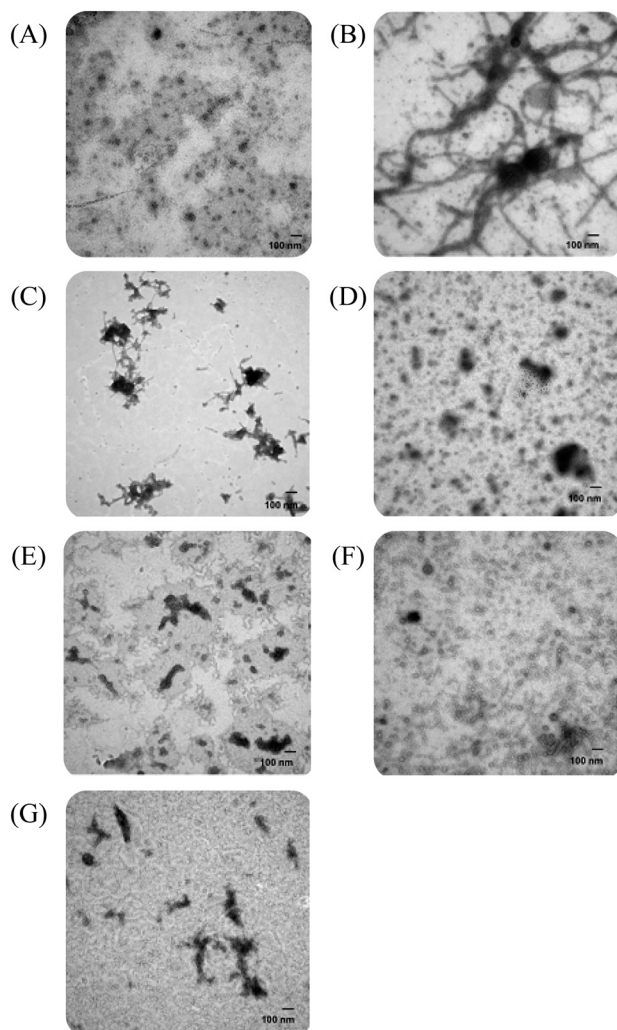
Fig. 6 Representative TEM images of Aβ42 (control) at t = 0 (A) and after 48 h of incubation at 37 °C alone (B) and in the presence of **2** (LDT544) (C), **3** (LDT636) (D), **5** (LDT638) (E), **7** (LDT640) (F), and **11** (LDT692) (G).

In vitro antioxidant activity

The antioxidant activity of cardanol derivatives **2–11** was assessed *in vitro* using the hydroxyl radical absorbance capacity (HORAC) assay. Based on the manufacturer's protocol, gallic acid, a naturally occurring triphenolic compound,[39,40] was used as an internal reference compound and the antioxidant activity is given as gallic acid equivalents (GAEs). Ferulic acid was also assayed as a reference antioxidant agent, as its radical scavenging properties have already been assessed as beneficial in protecting neuronal cells in an oxidative stress cell model.[41] Data listed in Table 1 show that all derivatives exerted an antioxidant activity close to or higher than that exerted by gallic acid (GAE values ≥ 1.49). Indeed, most derivatives performed similarly to ferulic acid as hydroxyl scavenging agents with GAE values ranging from 3.5 to 5.5. The best antiradical activity was shown by the morpholino derivative **7** (GAE of 9.73). Disappointingly, **7**

was devoid of any anticholinesterase activity. Conversely, compounds **5** and **11**, which are endowed with a good ChE inhibitory profile, performed as well as ferulic acid.

In vitro blood–brain barrier permeation assay

The *in vitro* BBB permeability of **2–11** was predicted by using the parallel artificial membrane permeability assay for the BBB (PAMPA–BBB), an efficient and simple method for evaluating BBB permeation at the early stage of development.[42] In this assay, porcine brain lipids are used as an artificial membrane to test the passive permeability of the tested compounds. Six commercial drugs (Table 2), whose central nervous system (CNS) availability is known, were used as standards to validate our in-house assay. Compounds labeled as CNS (+) should be able to cross the BBB by passive diffusion as their effective permeability (P_e) values are higher than that of CNS standard drugs (*i.e.*, tacrine, donepezil, rivastigmine).

The threshold to classify a compound as CNS (+) or CNS (−) was set at P_e = 5.96, which corresponds to that of CNS-permeable tacrine. In fact, negative controls (chlorothiazide, cefuroxime and furosemide) show P_e values substantially below this threshold. Compound **2** was not categorized because of biased results due to its low solubility in the assay medium. The results in Table 2 show that all the tested cardanol derivatives were predicted as CNS (+), with high P_e values. To note, the highest values are associated with **7**, carrying a morpholino moiety, which is known to confer favorable BBB permeation properties.[43] Hence, notwithstanding **7** being devoid of an anticholinesterase/anti-amyloid multifunctional profile, it might find further application as a centrally active radical scavenging agent.

Compounds **5** and **9**, endowed with concomitant cholinesterase/anti-amyloid/antioxidant activities, were among the most permeable compounds. Conversely,

Table 2 Prediction of BBB penetration of **2–11** and marketed drugs, expressed as P_e ± SEM (n = 2–3)

Compound	BBB penetration estimation	
	P_e ± SEM (10^{-6} cm s^{-1})	CNS (+/−)
LDT544 (**2**)	N.D.^{a}	
LDT636 (**3**)	9.6 ± 2.3	CNS+
LDT637 (**4**)	23.1 ± 2.4	CNS+
LDT638 (**5**)	19.5 ± 1.9	CNS+
LDT639 (**6**)	18.8 ± 8.6	CNS+
LDT640 (**7**)	32.0 ± 4.3	CNS+
LDT641 (**8**)	15.3 ± 3.5	CNS+
LDT642 (**9**)	39.3 ± 3.4	CNS+
LDT643 (**10**)	21.7 ± 5.2	CNS+
LDT692 (**11**)	12.0 ± 1.5	CNS+
Tacrine	5.96 ± 0.59	CNS+
Donepezil	21.49 ± 2.05	CNS+
Rivastigmine	20.0 ± 2.07	CNS+
Chlorothiazide	1.14 ± 0.53	CNS−
Cefuroxime	0.62 ± 0.16	CNS−
Furosemide	0.19 ± 0.07	CNS−

^{a} N.D. stands for not determined due to low solubility in the assay buffer.

compound **3** (P_e = 9.6 × 10^{-6} cm s^{-1}), with a diethylamino moiety, displays the lowest permeability among the series.

Antioxidant activity in SHSY-5Y cells

With all the *in vitro* characterization data in hand, the compounds that were deemed to have cholinesterase activity and anti-amyloid and antioxidant capacity, and showed positive PAMPA–BBB values progressed to the next stage of investigation (*i.e.*, cell culture experiments). *In vitro* experiments showed that **5** and **11** display an antioxidant activity similar to that of ferulic acid, together with a *h*BChE and *h*AChE inhibitory profile (Table 1), modulate amyloid aggregation, and are predicted to cross the BBB. For these reasons, we selected **5** and **11** to be further tested for their ability to protect neuronal cells from oxidative stress.

During AD pathology, the imbalance between the generation and detoxification of reactive oxygen species (ROS), referred to as oxidative stress, induces widespread damage by oxidizing lipids, proteins, and DNA.[44] Since neuronal membranes contain many polyunsaturated fatty acids, neurons are particularly vulnerable to free radical attacks. With oxidative stress being an early and prominent feature of AD,[45] it appears rational that antioxidants will be beneficial in the treatment of AD.[46] In this study, the SHSY-5Y human neuronal cell line was used to estimate the protective effects of **5** and **11** against ROS (Fig. 7). ROS

production induced by the organic peroxide *t*-BuOOH (TBH) was measured by using the cell-permeant probe 2′,7′-dichlorodihydrofluorescein diacetate (H$_2$DCFDA), which is de-esterified inside cells and converted to the highly fluorescent 2′,7′-dichlorofluorescein (DCF) upon oxidation. Trolox was used as an antioxidant reference compound. In the absence of oxidative stress, incubation with **5** and **11** did not affect significantly ROS levels. When cells were challenged with mild oxidative stress using 100 μM TBH for 30 min, an expected increase of intracellular ROS was observed (Fig. 7). Interestingly, 24 h pre-incubation with both **5** and **11** significantly reduced the intracellular ROS concentration ($p < 0.001$). Notably, at a 10 μM concentration, compounds **5** and **11** protected cells from oxidative stress in a similar fashion to 100 μM Trolox.[47] Thus, under these experimental conditions, **5** and **11** are more effective antioxidants than Trolox. In addition, they have been predicted to cross the BBB. This is particularly relevant, as failures of antioxidants in AD clinical studies have been at least partially attributed to their inability to cross the BBB after systemic administration.[48]

Toxicity in HepG2 cells

Therapy with tacrine, the first marketed ChE inhibitor, has been associated with a very high rate of serum enzyme elevations, which has been associated with liver injury.[49] Because of this side effect and the availability of other better tolerated ChEIs, tacrine is now no longer used. To this end, we preliminarily tested the hepatotoxicity of cholinesterase inhibitors **5** and **11** in cells from human hepatocellular carcinoma (HepG2) by the MTT assay (Fig. 8).

Data from Fig. 8 show that compounds **5** and **11** have no significant cytotoxic effect up to 10 μM. This reinforces the favorable early-tox profile of **5** and **11**.
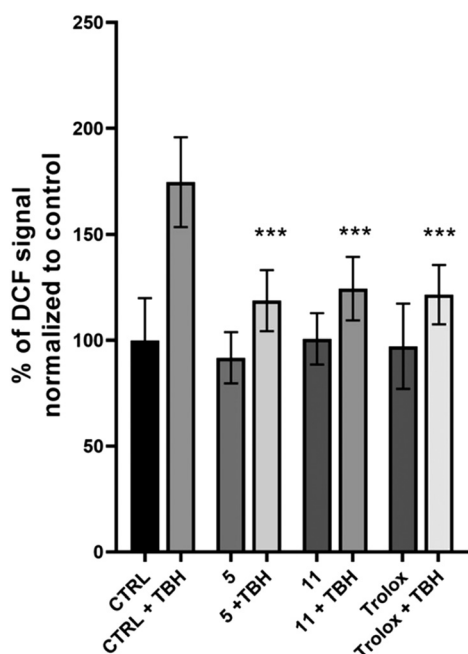
Fig. 7 Reactive oxygen species (ROS) determination in live SH-SY5Y cells. ROS were detected by staining the cells with H$_2$DCFDA. Cells were incubated for 24 h with compounds **5** and **11** (10 μM), Trolox (100 μM) or a vehicle (CTRL) and oxidative stress was detected in the presence and absence of 100 μM *t*-BuOOH (TBH) exposure. Data are presented as a percentage of DCF signal normalized to control. Error bars indicate ± SD. (*n* = 3); ***$P < 0.001$.
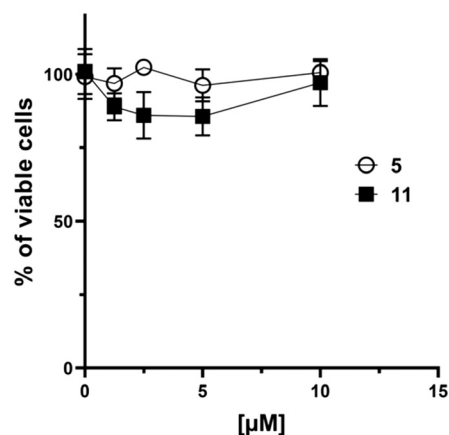
Fig. 8 Cell viability determined by the MTT assay. Human hepatocarcinoma cells (HepG2) were treated with **5** and **11** for 24 h at a concentration ranging from 1.25 μM to 10 μM. Data are presented as a percentage of viable cells in comparison with vehicle-treated controls. Error bars indicate ± SD; *n* = 3.

A plasma stability of **5**

B plasma stability of **11**
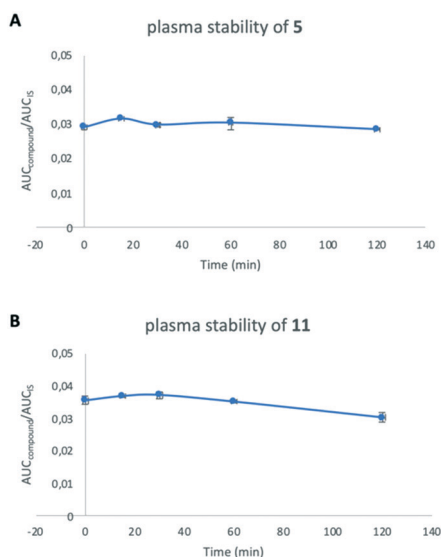
Fig. 9   Plasma stability of compounds **5** (A) and **11** (B).

Plasma stability and kinetic solubility

Considering that Mannich bases may be unstable, we further checked the plasma stability of **5** and **11**, as well as their solubility properties. Compounds **5** and **11** were stable in plasma over a 60-minute timeframe (Fig. 9). After 120 minutes, there were still 97 ± 1.4% of compound **5** and 85 ± 7.0% of compound **11**. Furthermore, we have shown experimentally that compounds **5** and **11** are soluble in 5% DMSO/PBS solution at a concentration <3.9 mM and <5 mM, respectively. Thus, **5** and **11** show favorable preliminary drug-likeness.

Conclusions

AD, which was initially thought to be a disease confined to Western countries, has now gone global, becoming a pressing worldwide challenge with no therapy available. Thus, there is a quest for treatments that are not only effective, but also accessible to the global patient population. The molecules reported herein were designed with these requirements in mind. Particularly, we aimed to expand the pharmacological profile of **1**, previously developed as a cholinesterase inhibitor and obtained from an inexpensive food waste material, *i.e.*, CNSL. Notably, by properly modifying the structure of **1**, we came up with **5** and **11**, which combine cholinesterase activity together with anti-amyloid and antioxidant capacity and potential higher synthetic accessibility than conventional drugs. With regards to the initial ADME/Tox evaluation, they were found potentially BBB permeable, plasma-stable, soluble and devoid of hepatotoxicity. Thus, we succeeded in identifying **5** and **11** as sustainable multifunctional cholinesterase inhibitors, modulating amyloid and oxidative cascades.

This work also provides initial clues into the development of cheap and effective antioxidants derived from CNSL which can be followed for further AD drug design and development.

Author contributions

Conflicts of interest

The authors declare that they have no known competing financial interests or personal relationships that could have appeared to influence the work reported in this paper.

Acknowledgements

References

1   C. Brayne and B. Miller, *Dementia and aging populations—A global priority for contextualized research and health policy*, Public Library of Science San Francisco, CA USA, 2017.

2   *Alzheimer's Dementia*, 2020, **16**, 391–460.

3   M. Mehta, A. Adem and M. Sabbagh, *J. Alzheimer's Dis.*, 2012, **2012**, 728983.

4   H. Wang and H. Zhang, *ACS Chem. Neurosci.*, 2019, **10**, 852–862.

5   A. A. de Paula, J. B. Martins, M. L. dos Santos, L. E. C. Nascente, L. A. Soares Romeiro, T. F. Areas, K. S. Vieira, N. F. Gambôa, N. G. Castro and R. Gargano, *Eur. J. Med. Chem.*, 2009, **44**, 3754–3759.

6   L. A. Soares Romeiro, J. L. da Costa Nunes, C. de Oliveira Miranda, G. S. H. R. Cardoso, A. S. de Oliveira, A. Gandini, T. Kobrlova, O. Soukup, M. Rossi, J. Senger, M. Jung, S. Gervasoni, G. Vistoli, S. Petralla, F. Massenzio, B. Monti and M. L. Bolognesi, *ACS Med. Chem. Lett.*, 2019, **10**, 671–676.

7   L. F. N. Lemes, G. de Andrade Ramos, A. S. de Oliveira, F. M. R. da Silva, G. de Castro Couto, M. da Silva Boni, M. J. R. Guimarães, I. N. O. Souza, M. Bartolini, V. Andrisano, P. Coelho do Nascimento Nogueira, E. Rocha Silveira, G. D. Brand, O. Soukup, J. Korábečný, N. C. Romeiro, N. G. Castro, M. L. Bolognesi and L. A. Soares Romeiro, *Eur. J. Med. Chem.*, 2016, **108**, 687–700.

8   A. Castro and A. Martinez, *Mini-Rev. Med. Chem.*, 2001, **1**, 267–272.

9   K. Ono, T. Hamaguchi, H. Naiki and M. Yamada, *Biochim. Biophys. Acta, Mol. Basis Dis.*, 2006, **1762**, 575–586.

10 D. A. Butterfield and D. Boyd-Kimball, *J. Alzheimer's Dis.*, 2018, **62**, 1345–1367.

11 C. Cheignon, M. Tomas, D. Bonnefont-Rousselot, P. Faller, C. Hureau and F. Collin, *Redox Biol.*, 2018, **14**, 450–464.

12 G. Caruso, S. F. Spampinato, V. Cardaci, F. Caraci, M. A. Sortino and S. Merlo, *Curr. Pharm. Des.*, 2019, **25**, 4771–4781.

13 O. Benek, J. Korabecny and O. Soukup, *Trends Pharmacol. Sci.*, 2020, **41**, 434–445.

14 D. Panek, T. Wichur, J. Godyń, A. Pasieka and B. Malawska, *Future Med. Chem.*, 2017, **9**, 1835–1854.

15 E. Viayna, N. Coquelle, M. Cieslikiewicz-Bouet, P. Cisternas, C. A. Oliva, E. Sánchez-López, M. Ettcheto, M. Bartolini, A. De Simone, M. Ricchini, M. Rendina, M. Pons, O. Firuzi, B. Pérez, L. Saso, V. Andrisano, F. Nachon, X. Brazzolotto, M. L. García, A. Camins, I. Silman, L. Jean, N. C. Inestrosa, J. P. Colletier, P. Y. Renard and D. Muñoz-Torrero, *J. Med. Chem.*, 2021, **64**, 812–839.

16 M. L. Bolognesi, A. Minarini, M. Rosini, V. Tumiatti and C. Melchiorre, *Mini-Rev. Med. Chem.*, 2008, **8**, 960–967.

17 T. Hamaguchi, K. Ono, A. Murase and M. Yamada, *Am. J. Pathol.*, 2009, **175**, 2557–2565.

18 K. Ono, L. Li, Y. Takamura, Y. Yoshiike, L. Zhu, F. Han, X. Mao, T. Ikeda, J. Takasaki, H. Nishijo, A. Takashima, D. B. Teplow, M. G. Zagorski and M. Yamada, *J. Biol. Chem.*, 2012, **287**, 14631–14643.

19 C. Rice-Evans, N. Miller and G. Paganga, *Trends Plant Sci.*, 1997, **2**, 152–159.

20 N. Meshginfar, H. Tavakoli, K. Dornan and F. Hosseinian, *Crit. Rev. Food Sci. Nutr.*, 2020, 1–10.

21 Y. Li, X. Qiang, L. Luo, X. Yang, G. Xiao, Q. Liu, J. Ai, Z. Tan and Y. Deng, *Eur. J. Med. Chem.*, 2017, **126**, 762–775.

22 H. Liu, X. Qiang, Q. Song, W. Li, Y. He, C. Ye, Z. Tan and Y. Deng, *Bioorg. Med. Chem.*, 2019, **27**, 991–1001.

23 M. Cerone, E. Uliassi, F. Prati, G. U. Ebiloma, L. Lemgruber, C. Bergamini, D. G. Watson, T. A. M. de Ferreira, G. S. H. R. Cardoso, L. A. Soares Romeiro, H. P. de Koning and M. L. Bolognesi, *ChemMedChem*, 2019, **14**, 621–635.

24 I. Kubo, S. Komatsu and M. Ochi, *J. Agric. Food Chem.*, 1986, **34**, 970–973.

25 R. Paramashivappa, P. P. Kumar, P. J. Vithayathil and A. Srinivasa Rao, *J. Agric. Food Chem.*, 2001, **49**, 2548–2551.

26 G. L. Ellman, K. D. Courtney, V. Andres Jr and R. M. Featherstone, *Biochem. Pharmacol.*, 1961, **7**, 88–95.

27 F. Prati, C. Bergamini, R. Fato, O. Soukup, J. Korábečný, V. Andrisano, M. Bartolini and M. L. Bolognesi, *ChemMedChem*, 2016, **11**, 1284–1295.

28 Q. Li, H. Yang, Y. Chen and H. Sun, *Eur. J. Med. Chem.*, 2017, **132**, 294–309.

29 G. Mushtaq, N. H. Greig, J. A. Khan and M. A. Kamal, *CNS Neurol. Disord.: Drug Targets*, 2014, **13**, 1432–1439.

30 U. Kosak, B. Brus, D. Knez, S. Zakelj, J. Trontelj, A. Pišlar, R. Šink, M. Jukič, M. Živin, A. Podkowa, F. Nachon, X. Brazzolotto, J. Stojan, J. Kos, N. Coquelle, K. Sałat, J. P. Colletier and S. Gobec, *J. Med. Chem.*, 2018, **61**, 119–139.

31 M. Hoffmann, C. Stiller, E. Endres, M. Scheiner, S. Gunesch, C. Sotriffer, T. Maurice and M. Decker, *J. Med. Chem.*, 2019, **62**, 9116–9140.

32 M. Ekholm, *J. Mol. Struct.: THEOCHEM*, 2001, **572**, 25–34.

33 J. Cheung, M. J. Rudolph, F. Burshteyn, M. S. Cassidy, E. N. Gary, J. Love, M. C. Franklin and J. J. Height, *J. Med. Chem.*, 2012, **55**, 10282–10286.

34 T. L. Rosenberry, X. Brazzolotto, I. R. Macdonald, M. Wandhammer, M. Trovaslet-Leroy, S. Darvesh and F. Nachon, *Molecules*, 2017, **22**, 2098.

35 V. L. Anderson and W. W. Webb, *BMC Biotechnol.*, 2011, **11**, 125.

36 C. Haass and D. J. Selkoe, *Nat. Rev. Mol. Cell Biol.*, 2007, **8**, 101–112.

37 D. E. Ehrnhoefer, J. Bieschke, A. Boeddrich, M. Herbst, L. Masino, R. Lurz, S. Engemann, A. Pastore and E. E. Wanker, *Nat. Struct. Mol. Biol.*, 2008, **15**, 558–566.

38 H. LeVine, *J. Alzheimer's Dis.*, 2004, **6**, 303–314.

39 B. Badhani, N. Sharma and R. Kakkar, *RSC Adv.*, 2015, **5**, 27540–27557.

40 B. Halliwell, J. M. Gutteridge and O. I. Aruoma, *Anal. Biochem.*, 1987, **165**, 215–219.

41 J. Kanski, M. Aksenova, A. Stoyanova and D. A. Butterfield, *J. Nutr. Biochem.*, 2002, **13**, 273–281.

42 L. Di, E. H. Kerns, K. Fan, O. J. McConnell and G. T. Carter, *Eur. J. Med. Chem.*, 2003, **38**, 223–232.

43 A. K. Ghose, T. Herbertz, R. L. Hudkins, B. D. Dorsey and J. P. Mallamo, *ACS Chem. Neurosci.*, 2012, **3**, 50–68.

44 X. Wang, W. Wang, L. Li, G. Perry, H. Lee and X. Zhu, *Biochim. Biophys. Acta*, 2014, **1842**, 1240–1247.

45 M. Rosini, E. Simoni, A. Milelli, A. Minarini and C. Melchiorre, *J. Med. Chem.*, 2014, **57**, 2821–2831.

46 G. Veurink, G. Perry and S. K. Singh, *Open Biol.*, 2020, **10**, 200084.

47 L. Pruccoli, F. Morroni, G. Sita, P. Hrelia and A. Tarozzi, *Antioxidants*, 2020, **9**, 551.

48 F. J. Pérez-Areales, M. Garrido, E. Aso, M. Bartolini, A. De Simone, A. Espargaró, T. Ginex, R. Sabate, B. Pérez, V. Andrisano, D. Puigoriol-Illamola, M. Pallàs, F. J. Luque, M. I. Loza, J. Brea, I. Ferrer, F. Ciruela, A. Messeguer and D. Muñoz-Torrero, *J. Med. Chem.*, 2020, **63**, 9360–9390.

49 P. B. Watkins, H. J. Zimmerman, M. J. Knapp, S. I. Gracon and K. W. Lewis, *JAMA*, 1994, **271**, 992–998.